

Simple method for static and dynamic analyses of guyed towers

H. Meshmesha[†]

Department of Civil and Environmental Engineering, University of Windsor, Ontario, Canada

K. Sennah[‡]

Department of Civil Engineering, 350 Victoria st., Ryerson University, Toronto, Ontario, Canada

J. B. Kennedy^{‡†}

Department of Civil and Environmental Engineering, University of Windsor, Ontario, Canada

(Received October 13, 2004, Revised October 5, 2005, Accepted April 17, 2006)

Abstract. The static and dynamic responses of guyed telecommunication towers can be determined by using two models, the space truss element model, and the equivalent beam-column element model. The equivalent beam-column analysis is based on the determination of the equivalent shear, torsion, and bending rigidities as well as the equivalent area of the guyed mast. In the literature, two methods are currently available to determine the equivalent properties of lattice structures, namely: the unit load method, and the energy approach. In this study, an equivalent beam-column analysis is introduced based on an equivalent thin plate approach for lattice structures. A finite-element modeling, using suitably modified ABAQUS software, is used to investigate the accuracy of utilizing the different proposed methods in determining the static and dynamic responses of a guyed tower of 364.5-meter high subjected to static and seismic loading conditions. The results from these analyses are compared to those obtained from a finite-element modeling of the actual structure using 3-D truss and beam elements. Good agreement is shown between the different proposed beam-column models, and the model of the actual structure. However, the proposed equivalent thin plate approach is simpler to apply than the other two approaches.

Keywords: communication towers; guyed; dynamics; seismic; finite-element; analysis.

1. Introduction

Guyed towers can be analyzed by the finite element technique using two different approaches. The first approach incorporates two-node 3-D truss elements with three degrees of freedom at each node to represent the exact shape of the guyed mast. The second approach utilizes a beam-column

[†] Passed away, Former Senior Structural Engineer, Bantrel, Calgary, AL, Canada

[‡] Associate Professor, Corresponding author, E-mail: ksennah@ryerson.ca

^{‡†} Emeritus and Distinguished Univ. Professor

model with two nodes and six degrees of freedom at each node which leads to significant reduction in the degrees of freedom as well as in the time used in the analyses. In both approaches, the base of the tower is modeled so that the translation degrees of freedom as well as the rotation about the axis along the height of the tower are prevented. Cables are modeled using 3-D cable elements with initial stress. Only few investigators have dealt with equivalent beam-column elements for guyed masts. Two studies were found in the literature, the first one was proposed by Kahla (1993) for several lacing towers. In his study, the equivalent beam-column properties of the mast were derived by using the unit load method to determine the displacements of its centroidal axis under axial, shear, bending and torsional loads, equating them to those obtained from a model beam analysis under the same forces. The same properties can be derived using an element flexibility matrix approach utilizing the principle of virtual work. The second method was proposed by Teughels and De Roeck (2000), where the strain energy in the discrete lattice cell was determined as a function of the truss forces and equated to the strain energy of the equivalent beam segment. From energy equivalence, the expressions for the equivalent stiffnesses of the discrete cell can be determined. Both of the above approaches require extensive and cumbersome analytical derivations. In the present study, the equivalent shear, torsion, and bending rigidities as well as equivalent area of the guyed mast are determined by replacing the bracing members of the discrete lattice cell by an equivalent thin plate, first used in bridge analysis by Kollbrunner and Basler (1969) for quasi-closed sections. Based on that, an equivalent beam-column element approach is presented. The proposed element is then calibrated and compared to models from previous modeling methods and the exact shape model for the static and dynamic responses of a high guyed tower.

2. Equivalent thin plate approach

In lattice structures, an equivalent thin plate, Fig. 1(b), with a constant thickness may be utilized to simplify the global analysis of guyed masts modeling. This approach is based on strain energy considerations in which the strain energy of the plate due to shear in the plate is equated to the strain energy in the truss elements. Following this concept, Kollbrunner and Basler (1969) were able to determine the following equivalent thicknesses of some semi-closed lattice walls shown in

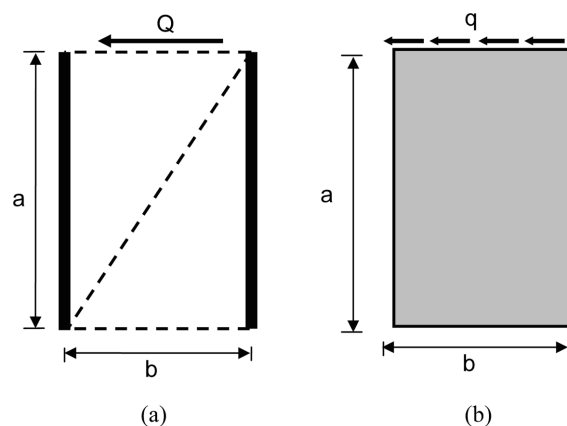


Fig. 1 Thin plate and a lattice cell

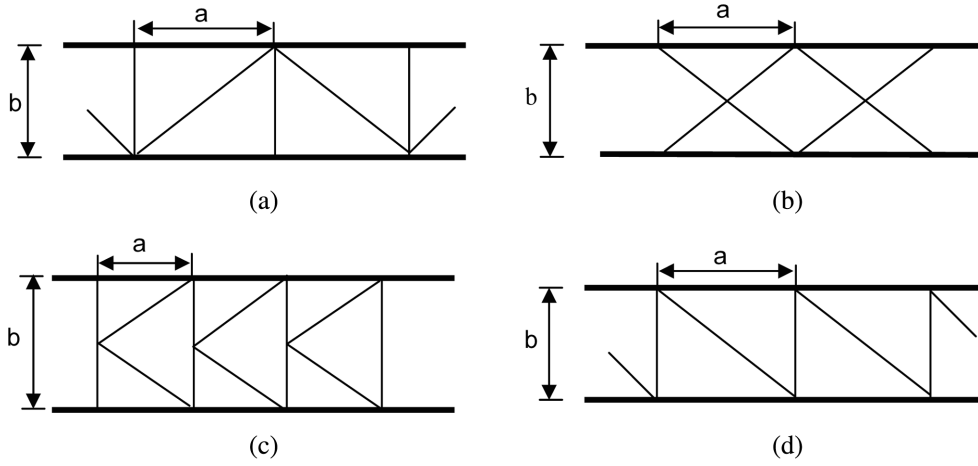


Fig. 2 Various lattice wall trusses

Figs. 2(a), (b), (c) and (d):

$$t_e = \frac{E}{G} \frac{ab}{\frac{d^3}{A_d} + \frac{a^3}{3} \left(\frac{2}{A_L} \right)} \quad \text{for truss a, (Fig. 2(a))} \quad (1)$$

$$t_e = \frac{E}{G} \frac{ab}{\frac{d^3}{2A_d} + \frac{a^3}{12} \left(\frac{2}{A_L} \right)} \quad \text{for truss b, (Fig. 2(b))} \quad (2)$$

$$t_e = \frac{E}{G} \frac{ab}{\frac{2d^3}{A_d} + \frac{b^3}{4A_v} + \frac{a^3}{12} \left(\frac{2}{A_L} \right)} \quad \text{for truss c, (Fig. 2(c))} \quad (3)$$

$$t_e = \frac{E}{G} \frac{ab}{\frac{d^3}{A_d} + \frac{b^3}{A_v} + \frac{a^3}{12} \left(\frac{2}{A_L} \right)} \quad \text{for truss d, (Fig. 2(d))} \quad (4)$$

where, t_e is the equivalent plate thickness; E is the modulus of elasticity; G is the shear modulus; a is the height of the panel; b is the width of the panel; d is the length of the diagonal member; and, A_d , A_v , and A_L are the cross sectional areas of diagonal, transverse, and leg (horizontal) members, respectively.

In the current study, the work was extended to obtain the following equivalent plate thicknesses for diagonal bracing, St.-Andrew's cross bracing and diamond bracing shown in Figs. 3(a), (b), and (c):

$$t_e = \frac{E}{G} \frac{ab}{\frac{d^3}{A_d} + \frac{a^3}{12} \left(\frac{2}{A_L} \right)} \quad \text{for diagonal bracing (Fig. 3(a))} \quad (5)$$

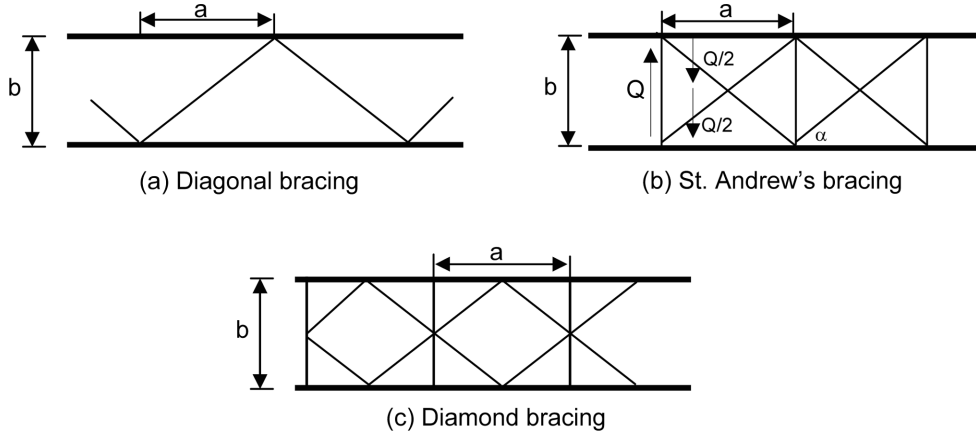


Fig. 3 Additional bracing configuration considered in the current study

$$t_e = \frac{E}{G} \frac{ab}{\frac{d^3}{2A_d} + \frac{a^3}{12} \left(\frac{2}{A_L} \right)} \quad \text{for St.-Andrew's bracing (Fig. 3(b))} \quad (6)$$

$$t_e = \frac{E}{G} \frac{ab}{\frac{4d^3}{A_d} + \frac{a^3}{12} \left(\frac{2}{A_L} \right)} \quad \text{for diamond bracing (Fig. 3(c))} \quad (7)$$

To illustrate Eqs. (5), (6), and (7), the derivation of the equivalent plate thickness for St. Andrew's cross bracing is presented. For the same applied shear force, Q , the strain energy for a thin plate wall with a thickness t_e shown in Fig. 1(b) can be expressed as following,

$$U_1 = \frac{q^2 ba}{2Gt_e} \quad \text{Where } U_1 \text{ is the strain energy and } q \text{ is the shear flow } (q = Q/b).$$

If the same shear force Q is applied to St. Andrew's lattice cell, the force in diagonal members would be

$$F_D = \frac{Q}{2\sin\alpha} \quad \text{as shown in Fig. 3(b), where } \sin\alpha = b/d. \text{ This is based on the assumption that all of}$$

the shear force will be carried by the diagonal members. This relation can be expressed as follows;

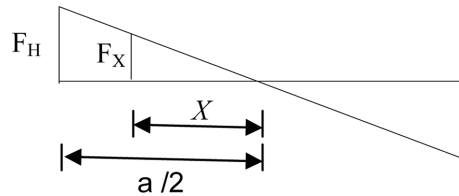


Fig. 4 Distribution of the force in horizontal members

$$F_D = \frac{qd}{2} \text{ where, } q = Q/b$$

The strain energy in two diagonal bracing members, U_D , due to the diagonal force F_D is;

$$U_D = 2 \times \frac{1}{2} \left(\frac{qd}{2} \right)^2 \frac{d}{EA_D} = \frac{q^2 d^3}{4 EA_D}$$

The maximum force in the horizontal member would be $F_H = \frac{Q \cos \alpha}{2 \sin \alpha} = \frac{qa}{2}$ where $\cos \alpha = a/d$.

The distribution of force along the horizontal member due to the effect of applied shear force is shown in Fig. 4. The strain energy in the two horizontal members, U_H , due to this distribution force is;

$$U_H = 4 \int_0^{a/2} \frac{qx^2}{2EA_L} dx = \frac{q^2 a^3}{12 EA_L}$$

The equivalent plate thickness can be calculated by equating the strain energy from the lattice cell with the one of thin plate as follows;

$$\frac{q^2 ba}{2Gt_e} = \frac{q^2 d^3}{4EA_D} + \frac{q^2 a^3}{12EA_L} \text{ from which the equivalent thickness of the thin plate can be obtained. Similar}$$

approach can be used for different bracing configurations.

3. Equivalent beam-column properties

To develop the equivalent properties of the mast, a triangular mast with solid round legs was considered as shown in Fig. 5. The equivalent plate thickness was determined first from Eqs. (1) to (7). The beam-column properties of the mast can be determined as follows:

Equivalent beam-column axial stiffness per unit length, EA_{eq} , for the guyed mast shown in Fig. 5 was directly determined by equating it to the sum of the axial stiffness of leg members per unit length, EA_{Legs} , and the axial stiffness of equivalent thin plates per unit length, EA_{plates} , so that:

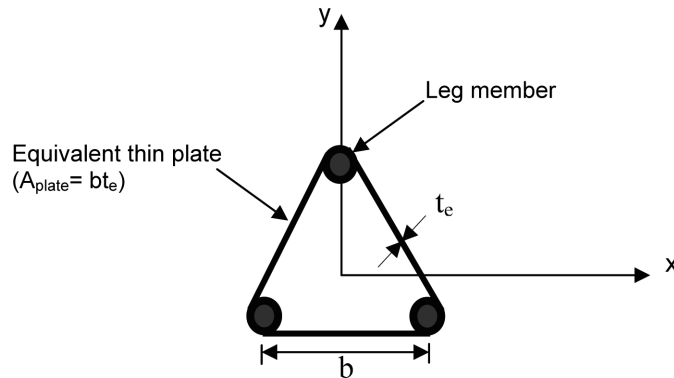


Fig. 5 Cross-section of a triangular guyed mast

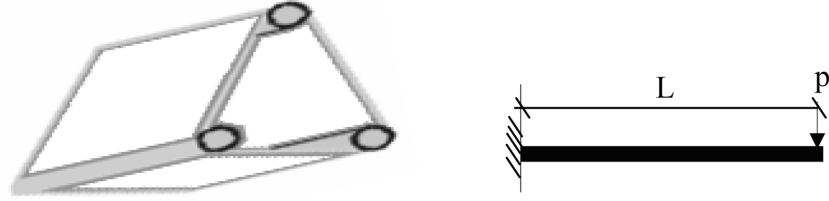


Fig. 6 Applied load for the equivalent beam column element and the thin plate element

$$EA_{eq} = E (A_{plates} + A_{legs}) \quad (8)$$

Where A_{eq} is the area of the equivalent beam-column section, A_{plates} is the area of the equivalent plates and, A_{legs} is area of the legs. The equivalent flexural stiffness, EI_{eq} , for the beam-column element (in x -direction, EI_{xx} , or in y -direction, EI_{yy}) was determined by computing the moment of inertia of the cross sectional area of both the legs and the plates about the x and the y -directions, respectively. Thus:

$$\begin{aligned} (EI_{eq})_{xx} &= (EI_{plates})_{xx} + (EI_{legs})_{xx} \quad \text{for } x\text{-direction} \\ (EI_{eq})_{yy} &= (EI_{plates})_{yy} + (EI_{legs})_{yy} \quad \text{for } y\text{-direction} \end{aligned} \quad (9)$$

Where I_{eq} , I_{plates} , and I_{legs} are moment of inertia of the equivalent beam-column section, the equivalent plates, and the legs, respectively. However, for simplicity, the flexural stiffness can be estimated from the leg members only since the contribution of the plates in flexural stiffness is insignificant compared to those of the leg members. The equivalent torsional rigidity, GJ_{eq} , of the beam-column element for the same angle of rotation per unit length and the same applied torque load on the mast, can be shown to be:

$$GJ_{eq} = \frac{b^2 GA_{plate}}{4} \quad (10)$$

Where b and A_{plates} are the width and the area of the equivalent plate, respectively, and $A_{plate} = bt_e$, and J_{eq} is the polar moment of inertia of the equivalent beam-column section.

The equivalent shear rigidity, GA_{eq} , for the beam-column element was deduced by applying Castigliano's theorem assuming the same displacement for the two types of modeling. From Fig. 6, it can be shown that, the displacements, δ at the tip of a beam with length, L , for a triangular tubular section and for the equivalent beam-column section, respectively, are:

$$\delta_{\text{tubular section}} = \frac{\sqrt{3} PL}{GA_{plates}} \quad (11)$$

$$\delta_{\text{Beam-column}} = \frac{10PL}{9GA_{eq}} \quad (12)$$

Where P is the applied shear, L is the length of the beam and A is the cross sectional area. Equating Eqs. (11), and (12), yields the equivalent shear rigidity, GA_{eq} :

Table 1 Equations for equivalent beam-column properties of a triangular cross section of the mast

Bracing pattern	Equivalent thickness (t_e)	EA	EI	GA	GJ
Fig. 1(a)	$\frac{E}{G} \frac{ab}{\frac{d^3}{A_d} + \frac{a^3}{12} \left(\frac{2}{A_L} \right)}$				
Fig. 1(b)	$\frac{E}{G} \frac{ab}{\frac{d^3}{2A_d} + \frac{a^3}{12} \left(\frac{2}{A_L} \right)}$				
Fig. 1(c)	$\frac{E}{G} \frac{ab}{\frac{2d^3}{A_d} + \frac{b^3}{4A_v} + \frac{a^3}{12} \left(\frac{2}{A_L} \right)}$				
Fig. 1(d)	$\frac{E}{G} \frac{ab}{\frac{d^3}{A_d} + \frac{b^3}{A_v} + \frac{a^3}{12} \left(\frac{2}{A_L} \right)}$	$E (A_{plates} + A_{legs})$	$EI_{eq} = EI_{plates} + EI_{legs}$	$\frac{10GA_{plates}}{9\sqrt{3}}$	$\frac{b^2GA_{plate}}{4}$
Fig. 3(a)	$\frac{E}{G} \frac{ab}{\frac{d^3}{A_d} + \frac{a^3}{12} \left(\frac{2}{A_L} \right)}$				
Fig. 3(b)	$\frac{E}{G} \frac{ab}{\frac{d^3}{2A_d} + \frac{a^3}{12} \left(\frac{2}{A_L} \right)}$				
Fig. 3(c)	$\frac{E}{G} \frac{ab}{\frac{4d^3}{A_d} + \frac{a^3}{12} \left(\frac{2}{A_L} \right)}$				

$$GA_{eq} = \frac{10GA_{plates}}{9\sqrt{3}} \quad (13)$$

The above equations are summarized in Table 1. The first step to determine the equivalent properties of the lattice cell is to determine the equivalent thin plate thickness and then use this thickness to determine the equivalent properties.

For the purpose of verification of this new analytical approach, the results from the finite element analysis using ABAQUS software, (Hibbitt *et al.* 2000) of the free vibration of a 3.65 m tested guyed tower model were compared to those obtained from laboratory model tests by Wahba (1999). Four clusters of guys support the tested tower model, with each cluster consisting of three guys radiating out symmetrically in plan. The pre-tension cable forces were 33 N in the first three clusters and 42 N in the top cluster. Fig. 7 shows the geometry of the experimental tower model. Both the mast and the guys' properties of the tower model are shown in Table 2. Views of the first three bending mode shapes are shown in Fig. 8. The comparison of the first three frequencies obtained experimentally and analytically, shown in Table 3, reveals good agreement.

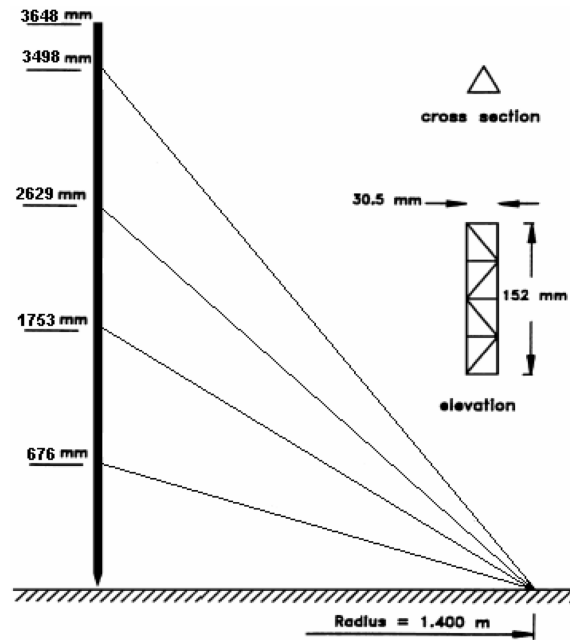


Fig. 7 Geometry of the experimental tower model

Table 2 Properties of the 3.65 m tested guyed tower model

Member	Legs	Diagonals	Horizontals	Guys
Area, m ²	7.9×10^{-6}	1.98×10^{-6}	1.98×10^{-6}	2.97×10^{-7} (Avg. area)
Modulus of elasticity, GPa			200	
Weight per meter of the mast (N/m)			0.65	

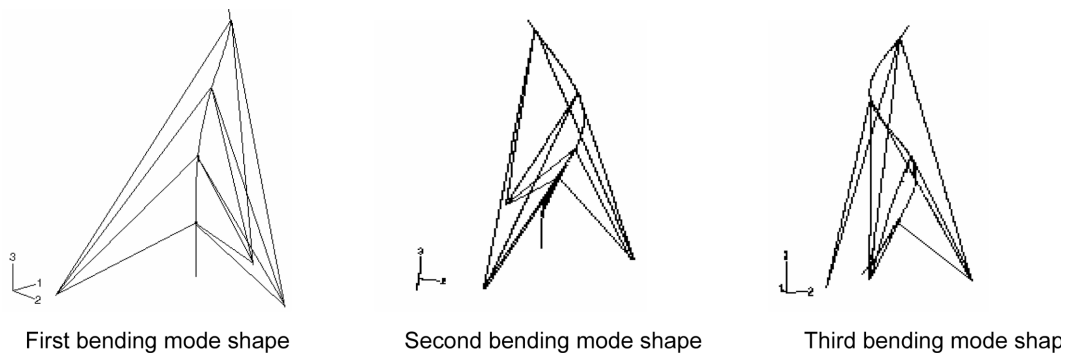


Fig. 8 First three bending mode shapes of the 3.65-m experimental tower model

4. Comparison with other beam-column models

A suitably modified ABAQUS software was used to investigate the accuracy of the proposed beam-column elements to determine the static, free-vibration and forced vibration responses of a

Table 3 Comparison of the experimental and analytical results for the 3.65 m guyed tower model

Study	Guy Mode 1	Bending Mode 1	Bending Mode 2
Experiment (Wahba 1999)	16 Hz	18.5 Hz	29 Hz
Present Study	17 Hz	17.65 Hz	28.9 Hz

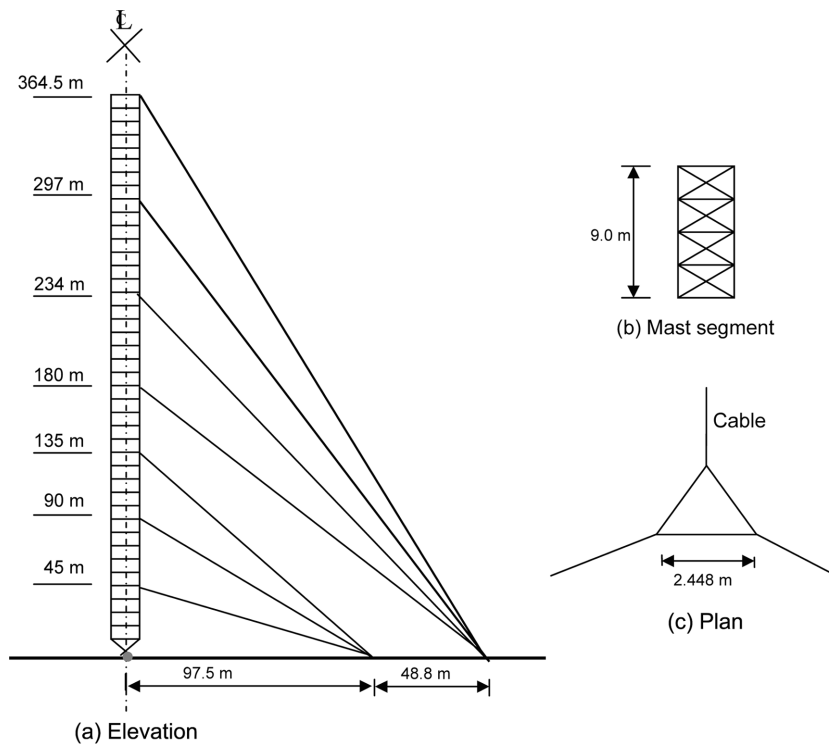


Fig. 9 Profile of the 364.5-m guyed tower

Table 4 Properties of the 364.5-m guyed tower

Member	Legs	Diagonals	Horizontals	Guys
Area, m ²	0.022	0.008	0.0014	0.0027
Modulus of elasticity, GPa			200	
Total weight per meter of the tower (kN/m)			6.65	
Weight per meter of the mast (kN/m)			4.65	

guyed tower, 364.5-meter high, subjected to static and to synchronous seismic loading conditions. Fig. 9 shows the profile of the guyed tower while Table 4 presents its properties. Two types of models were used in the analysis of the tower. The first model incorporated the proposed beam-column elements with equivalent properties derived from the unit load, the direct energy, and the equivalent thin plate approaches, while the second model utilized 3-D truss elements representing the actual diagonals and horizontals and 3-D beam elements, representing legs of the mast. The

Table 5 Equivalent properties of the 364.5-m by different beam column methods

Methods	A (m ²)	I (m ⁴)	J (m ⁴)	G (MPa)
Unit load	6.70×10^{-2}	6.62×10^{-2}	6.69×10^{-2}	2.63×10^9
Equivalent plate	6.90×10^{-2}	6.71×10^{-2}	5.10×10^{-2}	2.63×10^9
Direct energy	6.70×10^{-2}	9.88×10^{-2}	6.68×10^{-2}	2.57×10^9

values of the equivalent properties as obtained by these methods used are presented in Table 5. In both types of models, the guys were modeled as 3-D cable elements with two nodes and with each guy discretized into several elements according to its length. The materials were assumed to be linear elastic and the cables were initially pretensioned to approximately 10% of their ultimate strength.

5. Static analysis

A theoretical comparison between the exact shape model and the different beam-column models under the effect of applied vertical and lateral static loads at the top of the mast were obtained using the finite element software ABAQUS. Figs. 10(a) and (b) show the directions and the values of these applied loads for the space truss mast and the equivalent beam-column element where, two 10 kN loads were applied simultaneously in the gravitational and the lateral directions. Table 6 gives the base shear and the axial reactions at the base of the mast, showing good agreement between the different beam-column models and the exact shape model. The results based on the unit load and the equivalent plate methods are very close to the results of the exact shape method where the differences were 3.8% and 2.6% respectively. The reactions of one anchor at the same location for

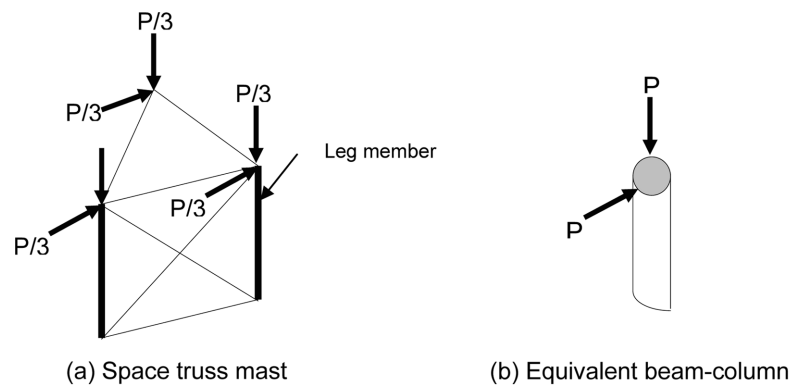


Fig. 10 Applied static loads

Table 6 Base shear and axial reaction at the base of the mast

Reaction	Model	Exact shape	Unit load	Equivalent plate	Direct energy
Base shear (kN)		17.32	16.66	16.88	14.83
Axial reaction (MN)		8.26	8.13	8.24	8.13

Table 7 Reactions in the three major directions at one anchor of the guyed tower

Reaction	Exact shape	Unit load	Equivalent plate	Direct energy
R_x (kN)	639	658	662	590
R_y (kN)	369	380	382	380
R_z (kN)	571	590	594	659

Table 8 Axial and lateral displacements at the top of the mast due to the applied static loads

Displacement	Model	Exact shape	Unit load	Equivalent plate	Direct energy
Lateral displacement (mm)		58	57.5	57.1	54.9
Axial displacement (mm)		136	127	123	127

the different models are compared in Table 7; whereas the displacements in the axial and the major y - y directions at the top of the mast are shown in Table 8. Again, the results show very good agreement.

6. Free vibration analysis

The natural frequencies of the tower have many mode types influencing each natural frequency. To determine all these mode types, two methods of modeling were used: the first one took into account the contribution of the guys' modes in the analysis by discretizing each guy into several elements. While in the second method, the modes of each guy were suppressed by reducing the number of degrees of freedom of each guy, treating it as one cable element. Applying the first method of modeling, it was found that the fundamental frequency of the tower is the one corresponding to the fundamental transverse mode of the longest guy cable as shown in Fig. 11. In addition, it can be observed that the first mode shape based on unit load and the equivalent thin plate models coincide with the one based on the exact shape model; however, a slight difference is observed between the mode shape based on the proposed direct energy method and the exact shape method. The second guys' mode shape resulted from the resonance of the upper guys also. Good

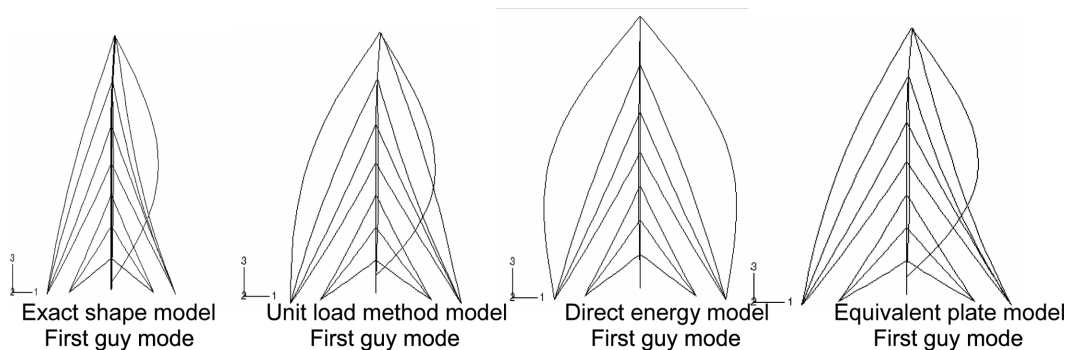


Fig. 11 First mode shape of guys of different models for the 364.5-m guyed tower

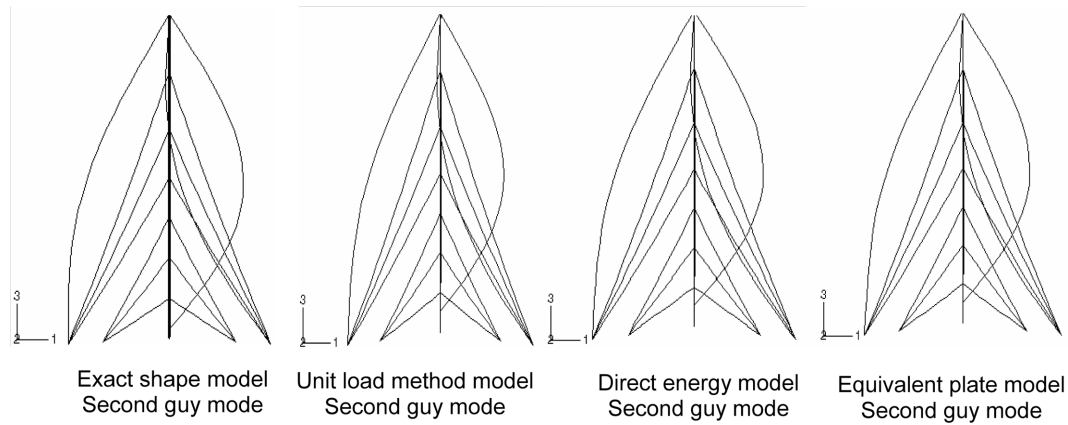


Fig. 12 Second mode shape of guys of different models for the 364.5-m guyed tower

Table 9 Frequencies of the first and second mode shapes of guys

Model frequency	Exact shape	Unit load	Direct energy	Equivalent plate
Frequency (Hz) Guy mode 1	0.163	0.165	0.165	0.165
Frequency (Hz) Guy mode 2	0.167	0.168	0.168	0.168

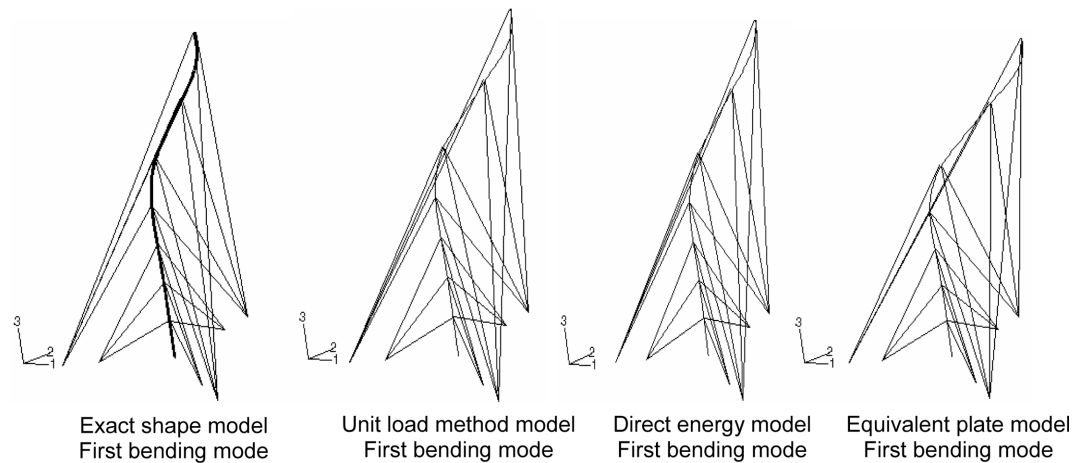


Fig. 13 First bending mode shape of different models for the 364.5-m guyed tower

agreement of the second mode shapes of the guys and frequencies obtained from the different proposed models and the exact shape model is observed as shown in Fig. 12. The frequencies of the first and second mode shapes of the guys are presented in Table 9.

To investigate the higher modes involving pure mast modes or the modes that have interactions between the guys and the mast, the eigenvalue problem should be solved for more than 100 modes until at least 90% of the total mass has been excited to vibrate. To investigate these modes, the

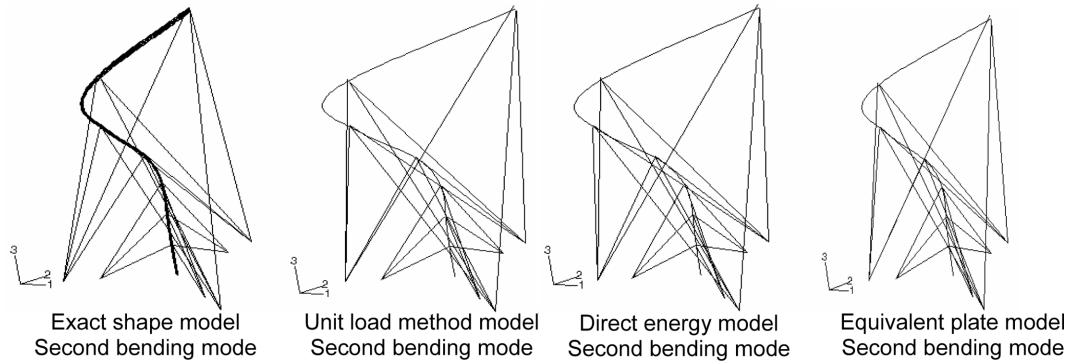


Fig. 14 Second bending mode shape of different models for the 364.5-m guyed tower

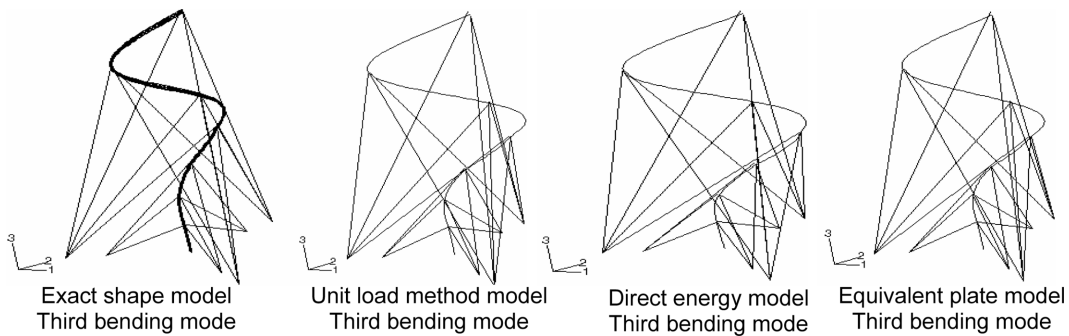


Fig. 15 Third bending mode shape of different models for the 364.5-m guyed tower

Table 10 The first three bending frequencies of the mast using different models

Model	Exact shape	Unit load	Direct energy	Equivalent plate
Frequency (Hz) Bending mode 1	0.451	0.471	0.481	0.464
Frequency (Hz) Bending mode 2	0.611	0.639	0.668	0.631
Frequency (Hz) Bending mode 3	0.876	0.919	0.978	0.906

second method of modeling mentioned earlier was used where the guy modes were suppressed by reducing the number of degrees of freedoms of the guys, modeling each guy with only one element. This procedure resulted in three major types of flexural vibration, namely: vibration due to the interaction between the upper guys and the mast where the resonance of the upper guys tends to bend the top of the mast as shown in Fig. 13; the second type of vibration, shown in Fig. 14 occurred due to the resonance of the lower guys. The third vibration type resulted from the interaction of the upper and lower guys with the mast producing the mode shape shown in Fig. 15. Again, the results show good agreement between the mode shapes based on the different equivalent beam-column elements and the exact shape model. However, the closest model to the exact shape model is the one that is based on the proposed equivalent plate approach as shown in Table 10.

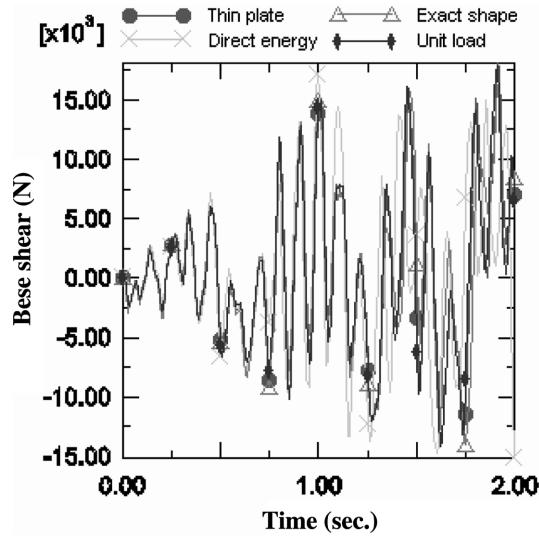


Fig. 16 Base shear force due to El Centro N-S earthquake

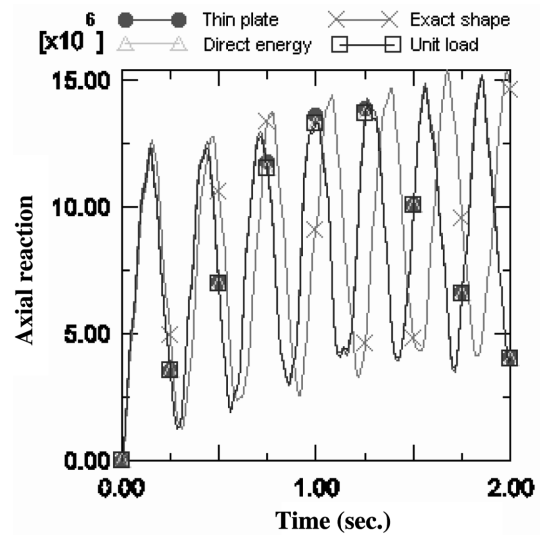


Fig. 17 Vertical reaction force due to El Centro N-S earthquake

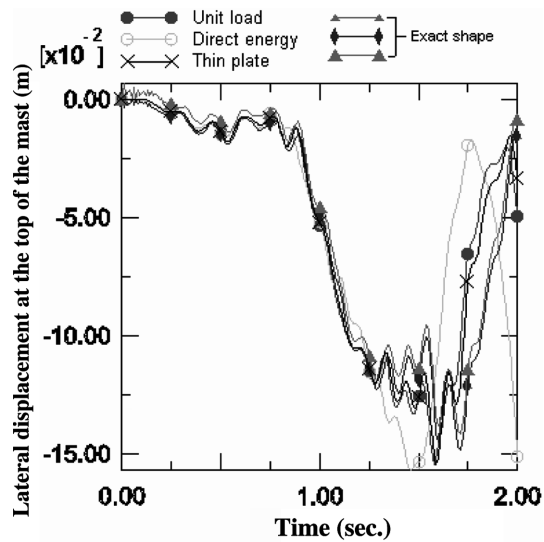


Fig. 18 Lateral displacement at the top of the mast due to El Centro N-S earthquake

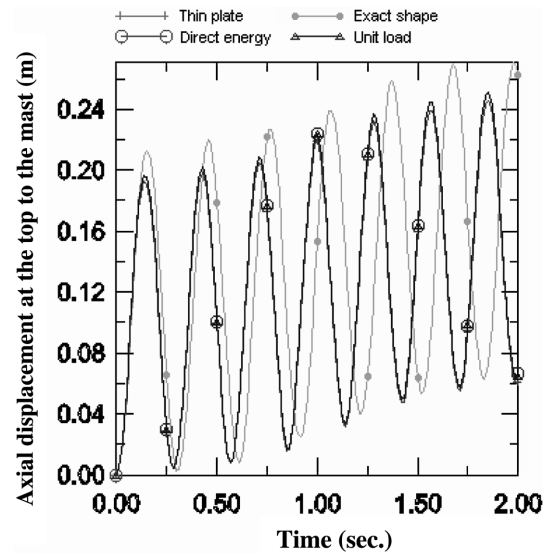


Fig. 19 Axial displacement at the top of the mast due to El Centro N-S earthquake

7. Forced vibration analysis

The response of the guyed tower was also determined for a seismic loading condition of a two-second event for the aforementioned models. The finite element software, ABAQUS, was used to obtain the system's response by direct integration in the time domain corresponding to El Centro N-S recorded data. The damping coefficients were considered zero in all models. The force was

applied at the base of the mast and at the guys' anchors simultaneously in the major direction y - y (Fig. 5). Fig. 16 shows the base shear force in the major direction y - y due to the seismic forces for all models and Fig. 17 presents the vertical reaction at the base of the tower. Good agreement can be observed between the results based on the different proposed beam-column models and the exact shape model. Fig. 18 shows the displacement in the major direction y - y at the top of the tower, while Fig. 19 shows the axial displacement at the top of the tower due to the applied seismic forces. Again, good agreement is shown between the results based on the various models.

8. Conclusions

A simple but realistic beam-column element for static, free, and forced vibration analyses of lattice structures and plate-like lattice structures was developed. The equivalent shear, torsion, and bending rigidities as well as the equivalent axial stiffness of the guyed mast were determined by replacing the bracing members of the mast by an equivalent thin plate. Comparison to results based on laboratory as well as on other beam-column elements show very good agreement with the proposed approach.

Acknowledgements

The support of the Natural Science and Engineering Research Council of Canada is greatly appreciated.

References

- Hibbitt, H.D., Karlsson, B.I. and Sorenson, J. (2000), *ABAQUS User's Manual Version 6.2*, Hibbitt, Karlsson, and Sorenson Inc., Providence, RI.
- Kahla, N.B. (1993), "Equivalent beam-column analyses of guyed towers", *Comput. Struct.*, **55**(4), 631-645.
- Kollbrunner, C.F. and Basler, K. (1969), *Torsion in Structures*, Springer-Verlag, Berlin, Germany.
- Teughels, A. and De Roeck, G. (2000), "Continuum models for beam and plate like lattice structures", *Fourth Int. Colloquium on Computation of Shell & Spatial Structures*, June 5-7, Chania - Crete, Greece.
- Wahba, Y.M. (1999), "Static and dynamic analysis of guyed antenna towers", Ph.D. Thesis, Department of Civil Engineering, University of Windsor, Windsor, Ontario, Canada.